Biochimica et Biophysica Acta 1790 (2009) 231–239

Contents lists available at ScienceDirect

Biochimica et Biophysica Acta

journal homepage: www.elsevier.com/locate/bbagen

Structural and catalytic roles of residues located in β13 strand and the following β-turn loop in *Fibrobacter succinogenes* 1,3-1,4-β-D-glucanase

Yu-Shiun Lin [a], Li-Chu Tsai [b], Shu-Hua Lee [a], Hanna S. Yuan [c], Lie-Fen Shyur [a,*]

[a] *Agricultural Biotechnology Research Center, Academia Sinica, Nankang, Taipei 115, Taiwan, ROC*
[b] *Department of Molecular Science and Engineering, National Taipei University of Technology, Taiwan, ROC*
[c] *Institute of Molecular Biology, Academia Sinica, Taiwan, ROC*

ARTICLE INFO

Article history:
Received 3 September 2008
Received in revised form 15 December 2008
Accepted 29 January 2009
Available online 11 February 2009

Keywords:
1,3-1,4-β-D-glucanase
Fibrobacter succinogenes
Catalytic efficiency
Comparative energy $\Delta\Delta G_b$
Structural modeling

ABSTRACT

Background: Fibrobacter succinogenes 1,3-1,4-β-D-glucanase (Fsβ-glucanase) is the only naturally occurring circularly permuted β-glucanase among bacterial glucanases with reverse protein domains. We characterized the functional and structural significance of residues 200–209 located in the domain B of Fsβ-glucanase, corresponding to the major surface loop in the domain A region of *Bacillus licheniformis* glucanase.
Methods: Rational design approaches including site-directed mutagenesis, initial-rate kinetics, and structural modeling analysis were used in this study.
Results: Our kinetic data showed that D202N and D206N exhibited a 1.8- and 1.5-fold increase but G207N, G207−, F205L, N208G and T204F showed a 7.0- to 2.2-fold decrease, in catalytic efficiency (k_{cat}/K_M) compared to the wild-type enzyme. The comparative energy $\Delta\Delta G_b$ value in individual mutant enzymes was well correlated to their catalytic efficiency. D206R mutant enzyme exhibited the highest relative activity at 50 °C over 10 min, whereas K200F was the most heat-sensitive enzyme.
Conclusions: This study demonstrates that Phe205, Gly207, and Asn208 in the Type II turn of the connecting loop may play a role in the catalytic function of Fsβ-glucanase.
General significance: Residues 200–209 in Fsβ-glucanase resided at the similar structural topology to that of *Bacillus* enzyme were found to play some similar catalytic function in glucanase.

1. Introduction

1,3-1,4-β-D-Glucanase or lichenase (1,3-1,4-β-D-glucan 4-glucanohydrolase, EC 3.2.1.73) is an endo-glycosidase that specifically cleaves β-1,4-glycosidic bonds in 3-*O*-substituted glucopyranose units through a double-displacement reaction assisted by general acid–base catalysis [1]. The natural substrates for this enzyme are β-glucans from grain endosperm cell walls or lichenan from the Iceland moss *Cetraria islandica*. Structurally, these substrates are linear homopolymers of glucose molecules linked via β-1,3- and β-1,4-glycosidic bonds at a ratio of ~1:2.5 [2,3]. When the substrates are hydrolyzed by 1,3-1,4-β-D-glucanase, trisaccharide 3-*O*-β-cellobiosyl-D-glucopyranose and tetrasaccharide 3-*O*-β-cellotriosyl-D-glucopyranose are the major products [4]. Various 1,3-1,4-β-D-glucanase genes from bacterial origins, including different *Bacillus* species [5–10], *Fibrobacter succinogenes* [11], *Ruminococcus flavefaciens* [12], and *Clostridium thermocellum* [13], and from higher plants such as barley [14,15], have been isolated, cloned and characterized. The microbial glucanases are classified as members of glycosyl hydrolase family 16 with a β-jellyroll structure, whereas the plant 1,3-1,4-β-D-glucanases belong to family 17 with a $(\beta/\alpha)_8$ three-dimensional structure. In general, the bacterial 1,3-1,4-β-D-glucanases are intrinsically more thermostable than the plant enzymes, and are important biotechnological aids in the brewing industry for reducing viscosity during mashing [16,17], and in the animal feeds industry for improving the digestibility of a plant-based diet [17,18].

Among bacteria that secrete 1,3-1,4-β-D-glucanase, *F. succinogenes* plays a major role in plant fiber degradation in the rumen of most livestock species. The protein sequence (349 amino acids; gene accession number: M33676) of *F. succinogenes* glucanase (Fsβ-glucanase) contains two highly conserved domains (A and B) and is circular permutated as well as oriented in a reverse order (B to A) to that of other 1,3-1,4-β-D-glucanases (A to B) from different origins [11,19–21]. Moreover, Fsβ-glucanase contains a five PXSSSS (P: proline; S: serine; X: possibly any amino acid) repeated segment and a basic terminal domain (BTD) rich in positively charged amino acids at its C terminus, which is not observed in other bacterial or fungal 1,3-1,4-β-D-glucanases [11,22]. Recently, we observed that a truncation on the C-terminal region containing the quintet repeat and BTD domain can greatly increase the specific activity and thermotolerance of Fsβ-glucanase [22]. In our previous studies of Fsβ-glucanase, we also demonstrated that Glu56, Asp58 and Glu60 residues played important role(s) in the catalysis of Fsβ-glucanase

* Corresponding author. Tel./fax: +886 2 2651 5028.
E-mail address: lfshyur@ccvax.sinica.edu.tw (L.-F. Shyur).

0304-4165/$ – see front matter © 2009 Elsevier B.V. All rights reserved.
doi:10.1016/j.bbagen.2009.01.013

[23], and Trp54, Trp141, Trp148 and Trp203 are crucial residues for maintaining structural integrity in the substrate-binding cleft and for the catalytic efficiency of the enzyme [24]. However, issues concerning the structural and functional relation of catalysis in Fsβ-glucanase as well as specific amino acids involving in substrate binding still remain to be further clarified.

Recently, we solved the crystal structure of TFsβ-glucanase, a truncated form of Fsβ-glucanase, using the multiple-wavelength anomalous dispersion (MAD) method [21]. The crystal structure of TFsβ-glucanase in complex with β-1,3-1,4-cellotriose (CLTR), a major product of the enzyme reaction, was also elucidated [25]. The TFsβ-glucanase is composed mainly of two antiparallel β-sheets with seven and eight strands arranged on top of each other to form a jellyroll β-sandwich structure (Fig. 1A). The substrate-binding site in the enzyme was located in a channel of approximately 25 Å long at the concave side of the protein molecule, which could accommodate five glucopyranose residues. The amino acid residues from Lys200 to Thr204 were located at the C-terminal end of strand β13, and residues from Phe205 to Arg209 followed in a β-turn loop connecting strands β13 and β14 and located at up-right of the concave side of the enzyme

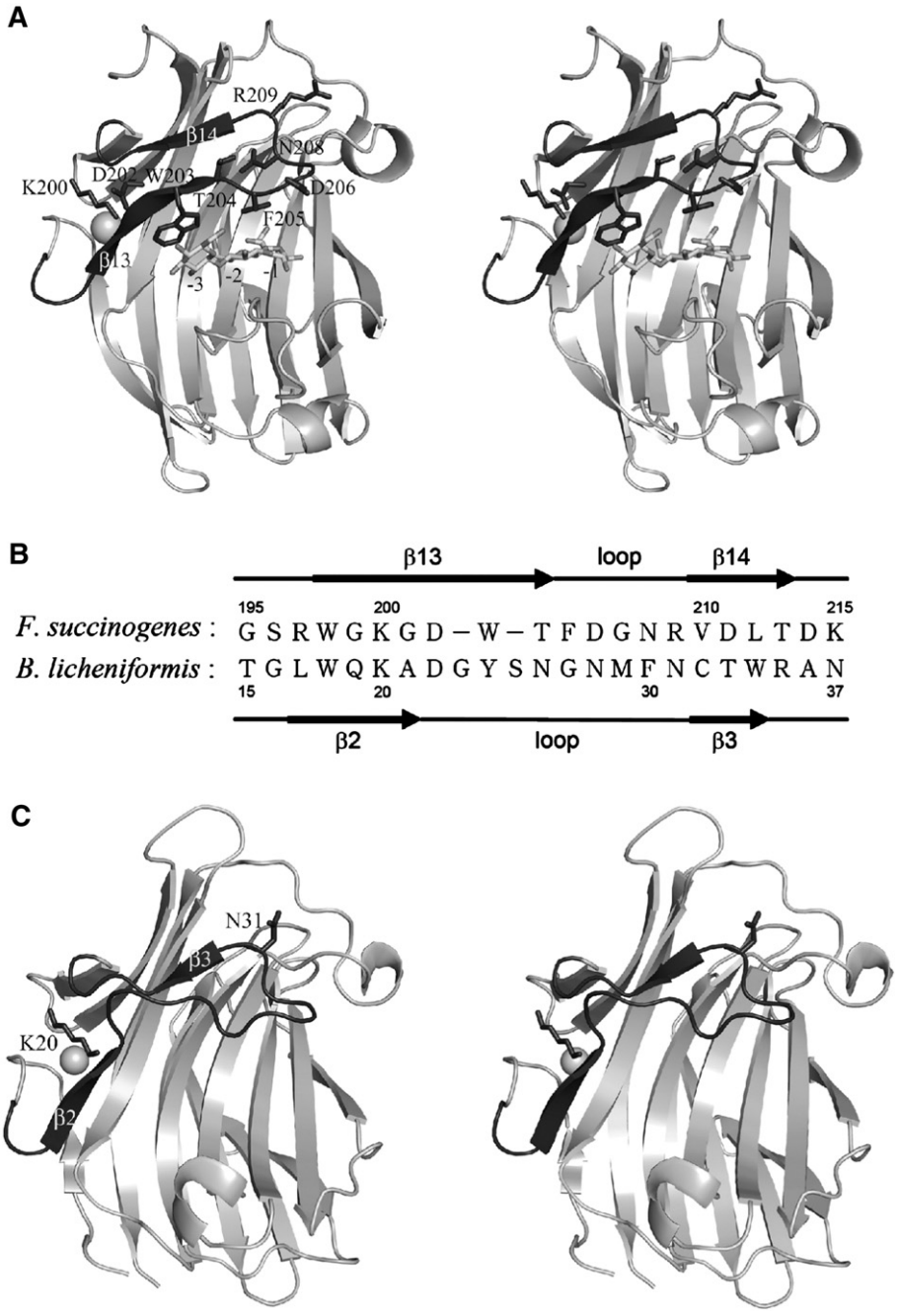

Fig. 1. (A) A ribbon drawing of the structure of truncated *Fibrobacter succinogenes* 1,3-1,4-β-D-glucanase (TFsβ-glucanase) in complex with β-1,3-1,4-cellotriose (CLTR). The overall topology of the TFsβ-glucanase–CLTR complex consists mainly of two eight-stranded anti-parallel β-sheets arranged in a jellyroll β-sandwich, and both β-sheets are twisted and bent, which results in a convex and a concave side of the molecule. The sugar product β-1,3-1,4-cellotriose is labeled as −3 to −1 (−1 is the reducing end). The calcium ion is displayed as a ball located on the convex side of the protein. (B) Structure-assisted sequence alignment of 1,3-1,4-β-D-glucanases from *F. succinogenes* and *B. licheniformis* was performed with use of ALSCRIPT [34]. Residues 200-209 located in the C-terminal half of strand β13 and the following loop to connect strand β14 of Fsβ-glucanase were related to the residues 20–31 located in the loop region between strands β2 and β3 in *B. licheniformis* 1,3-1,4-β-D-glucanase. (C) A ribbon drawing of *B. licheniformis* 1,3-1,4-β-D-glucanase structure showing the sequence of Lys20–Asn31, which forms a surface loop connecting β2 and β3 and covers the partial carbohydrate-binding cleft of the enzyme [27].

Table 1
Oligonucleotide primers for site-directed mutagenesis

Mutants	Sequences of mutagenic primers
K200F	5′-CCCGCTGGG GC**TT**CGGTGACTGGAC-3′
K200M	5′-CCCGCTGGGGCA**TG**GGTGACTGGAC-3′
G201S	5′-CCGCTGGGGCAAG**TC**TGACTGGACATTTG-3′
D202L	5′-GGGGCAAGGGT**CT**CTGGACATTTGAC-3′
D202N	5′-GGGGCAAGGGT**AA**CTGGACATTTG-3′
T204F	5′-GGCAAGGGTGACTGG**TTC**TTTGACGGTAACC-3′
F205L	5′-GGTGACTGGACATT**G**GACGGTAACCG-3′
D206M	5′-GGTGACTGGACATTT**ATG**GGTAACCGTGTCG-3′
D206N	5′-GGTGACTGGACATTT**A**ACGGTAACCGTGTCG-3′
D206R	5′-GACTGGACATTT**CG**CGGTAACCGTGTCG-3′
G207N	5′-GGACATTTGAC**AA**TAACCGTGTCGACC-3′
G207–	5′-GGACATTTGAC–––AACCGTGTCGACC-3′
N208G	5′-GGACATTTGACGGT**GG**CCGTGTCGACC-3′
R209M	5′-GACATTTGACGGTAAC**ATG**GTCGACCTCACCGAC-3′

(Fig. 1A) [25]. Amino acid sequence alignment of Fsβ-glucanase with 1,3-1,4-β-D-glucanase from *Bacillus licheniformis* (243 amino acids; gene accession number: X57279) [26] showed that the residues between Lys200 and Arg209 of Fsβ-glucanase corresponded to the sequence ^{20}KADGYSNGNMFN^{31} found in *B. licheniformis* 1,3-1,4-β-D-glucanase (Fig. 1B). Fig. 1C shows that the sequence between Lys20 and Asn31 in *B. licheniformis* 1,3-1,4-β-D-glucanase forms part of a surface loop, connecting strands β2 and β3, that covers the partial carbohydrate-binding cleft of the enzyme [26,27]. An alanine scanning mutagenesis study for the role of the surface loop residues in *B. licheniformis* 1,3-1,4-β-D-glucanase in substrate binding and stability have indicated that most mutations in the loop region affected enzyme kinetic properties through directly removing an amino acid side chain involved in substrate binding or in structural packing of the protein, or through indirectly local rearrangements in the protein structure [27]. Hence, we predicted that the corresponding residues Lys200 to Arg209 in Fsβ-glucanase might play important role (s) in substrate binding or enzyme stability, and the amino acid residues were selected to be investigated in this report for their functional and structural significance in the enzyme by rational design approaches, including site-directed mutagenesis along with initial rate kinetics; results were analyzed and explained by the three-dimensional structure and structural modeling of the wild-type and mutant enzymes.

2. Materials and methods

2.1. Bacterial strains, culture medium, and expression vector

The plasmid pET26b(+) (Novagene, Madison, WI) was used as the expression vector for glucanase in *Escherichia coli* cells. *E. coli* XL1-Blue was used for plasmid propagation and isolation, and *E. coli* BL21 (DE3) was used for protein expression and purification. Transformed *E. coli* cells were grown in Lubia–Bertani (LB) medium containing 30 μg/mL kanamycin at 37 °C.

2.2. Site-directed mutagenesis

The plasmid pFsNcE carrying *F. succinogenes* 1,3-1,4-β-D-glucanase gene in the pET26b(+) vector as described [23] was used as the template for site-directed mutagenesis by a PCR-based method. The selected amino acid residues and the mutant enzyme design are shown in Table 1. To obtain the desired mutations, pairs of complementary mutagenic primers were synthesized to mutate Lys200→Phe or Met, Gly201→Ser, Asp202→Leu or Asn, Thr204→Phe, Phe205→Leu, Asp206→Met, Asn or Arg, Gly207→Asn or deleted, Asn208→Gly, Arg209→Met (Table 1). Each PCR reaction mixture contained 10 mM KCl, 10 mM $(NH_4)_2SO_4$, 20 mM Tris–HCl (pH 8.8), 2 mM $MgSO_4$, 0.1% Triton® X-100, 0.1 mg/mL nuclease-free bovine serum albumin (BSA), 40 ng of DNA template, 0.2 mM dNTPs, 0.25 μM of each set of complementary primers, and 2.5 U of *PfuTurbo* DNA polymerase (Stratagene, La Jolla, CA).

The mutagenic PCR mixture was first reacted at 95 °C for 2 min, followed by 16 cycles at 55 °C for 1 min, 68 °C for 13 min, and 95 °C for 45 s on a thermocycler (TGradient 96, Biometra GmbH, Germany). The resulting products were incubated with 10 U of Dpn I at 37 °C for 1 h to digest the DNA template and then transformed into *E. coli* XL1-Blue supercompetent cells by the heat pulse method (Stratagene, CA). Appropriate volumes of each transformation mixture were plated on LB agar plate containing 30 μg/mL kanamycin at 37 °C. Colonies were selected from plates randomly and amplified at 37 °C for 16 h in 10 mL LB/kanamycin liquid media. Successful results of site-directed mutagenesis experiments were confirmed by DNA sequencing. For the over-expression of mutant enzymes, plasmids bearing the desired mutation were transformed into *E. coli* BL21 (DE3) by electroporation on an *E. coli* pulser (Bio-Rad, CA).

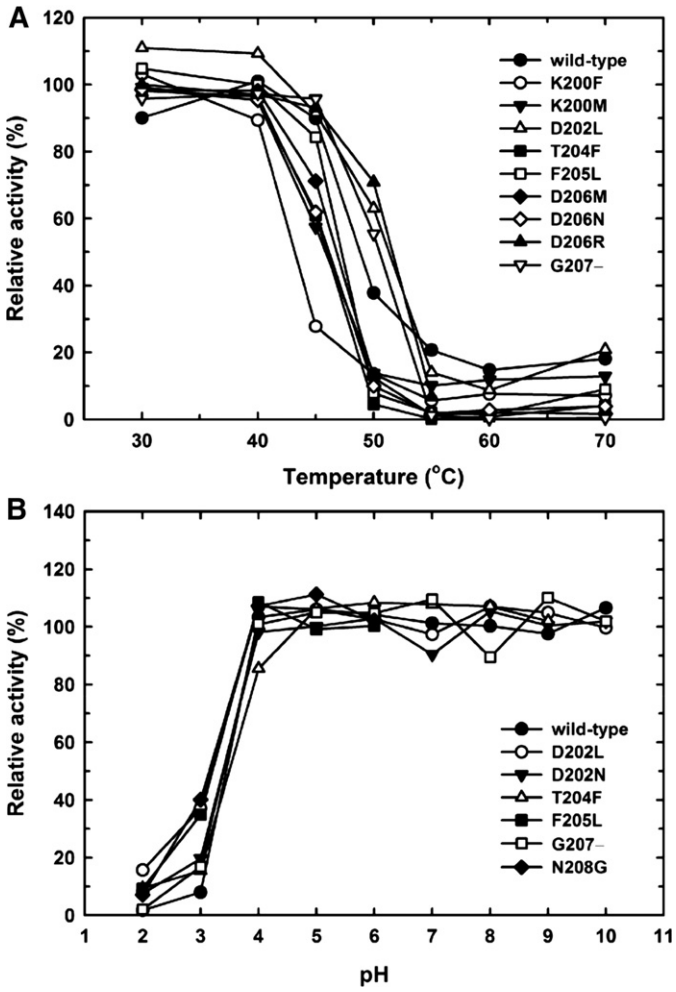

Fig. 2. Effects of temperature and pH on the enzymatic activity of wild-type and mutant *F. succinogenes* 1,3-1,4-β-D-glucanases. (A) Each enzyme was incubated for 10 min at 30, 40, 45, 50, 55, 60 and 70 °C, respectively, in 50 mM sodium citrate buffer (pH 6.0), 50 mM sodium phosphate buffer (pH 7.0) or 50 mM Tris–HCl buffer (pH 8.0) prior to activity assays. (B) Each enzyme was incubated at room temperature for 1 h in buffers with pH values ranging from pH 2 to 10. Different buffer solutions were prepared for this study, including 50 mM glycine–HCl (pH 2 and 3), 50 mM sodium citrate (pH 4, 5, and 6), 50 mM sodium phosphate (pH 7) and 50 mM Tris–HCl (pH 8, 9 and 10). Enzymatic activities were measured at the optimal temperature and pH of each individual enzyme immediately after incubation, and relative activity was expressed as percentage of the native enzyme activity under optimal assay conditions. Each assay was performed in triplicate.

2.3. Expression and purification of mutant enzymes

The *E. coli* BL21 (DE3) cells harboring the plasmid encoded for the mutant Fsβ-glucanase were grown at 33 °C in 2 L of LB/kanamycin with vigorous shaking until the OD_{600} reached about 0.6. Protein expression was then induced by the addition of 1 mM isopropyl-β-D-thiogalactopyranoside (IPTG) to the culture for a further 16 h at 33 °C. The supernatant, containing expressed proteins, was harvested from the culture medium by centrifugation, and then 1 mM phenylmethanesulfonyl fluoride and 1 μg/mL leupeptin were added to avoid enzymatic degradation. Subsequently, the supernatant was concentrated to about 100 mL by use of a Pellicon™-2 Mini Cassette concentrator with a Biomax™ 8-K filter (Millipore, Bedford, MA). The concentrate was dialyzed against 50 mM sodium phosphate buffer (SPB; pH 8.0) at 4 °C, and then adjusted to contain 10 mM imdazole and 0.3 M NaCl. The resulting protein solution was applied to a 1.5×12 cm Ni-NTA affinity column pre-equilibrated with 50 mM SPB (pH 8.0) containing 10 mM imidazole and 0.3 M NaCl. The column was washed with a 10-fold column volume of 50 mM SPB (pH 8.0) containing 20 mM imidazole and 0.3 M NaCl, followed with a linear gradient of 20–250 mM imidazole in the same buffer for protein elution. The eluent was collected as 2-mL fractions by a fraction collector (Gilson, WI). Aliquots of selected fractions were examined on 12.5% SDS-PAGE and zymogram analysis to monitor the protein purity and glucanase activity [23]. Protein fractions of more than 95% purity were dialyzed against 50 mM SPB (pH 7.0) at 4 °C, concentrated and then stored with the addition of 10% glycerol at −20 °C. The protein concentration was determined by the Bradford method (Bio-Rad) with BSA used as the standard.

2.4. Zymography analysis

The enzymatic activities of the mutant forms of Fsβ-glucanase were detected by zymography as previously documented [24]. A 12.5% SDS-polyacrylamide gel containing 0.1% lichenan was prepared. Protein samples were pre-treated with sample buffer containing 1% SDS and 2.5% β-mercaptoethanol at 90 °C for 10 min. After electrophoresis, the gel was rinsed with 25% isopropanol in 50 mM SPB (pH 7.0) twice for 20 min to remove SDS, and then equilibrated in 50 mM SPB (pH 7.0). Afterward, the gel was stained with Congo red solution (0.5 mg/mL) at an ambient temperature for 20 min. The proteins with 1,3-1,4-β-D-glucanase activity were visualized as transparent bands under staining.

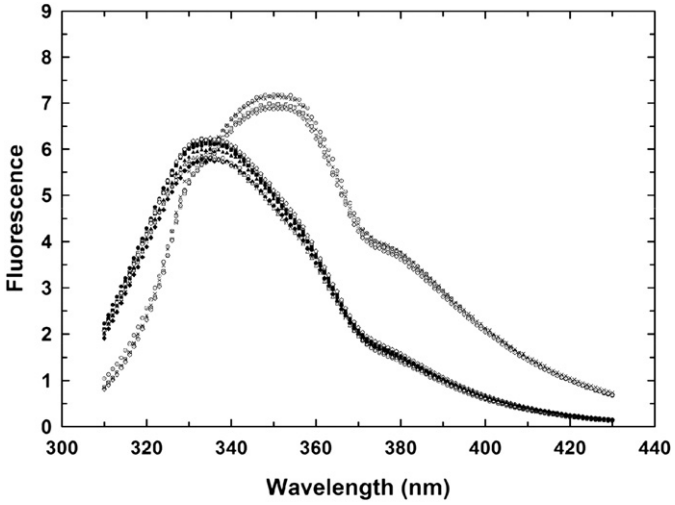

Fig. 3. Fluorescence emission spectra of wild-type and mutant *F. succinogenes* 1,3-1,4-β-D-glucanases. The fluorescence emission spectra of native, 8 M urea-denatured, and the denatured-renatured Fsβ-glucanase enzymes were quantitatively determined upon excitation at 295 nm using a spectrofluorometer. Each enzyme was measured at a concentration of 20 μg/mL in 50 mM sodium phosphate buffer (pH 7.0), or in 8 M urea-phosphate buffer. Fluorescence emission spectra of the native form of wild-type (○), D202L (□), F205L (◇), and N208G (△), denatured form of wild-type (⊙), D202L (⊡), F205L (◈), and N208G (⨯), and the denatured-renatured wild-type (●), D202L (■), F205L (◆), and N208G (▲) enzymes are presented.

2.5. Kinetic analysis

The enzymatic activities of the purified mutant 1,3-1,4-β-D-glucanases were measured by determining the rate of reducing sugar production from the hydrolysis of the substrate lichenan. Reducing sugars were quantified by the use of 3,5-dinitrosalicylic acid reagent [28] with glucose used as the standard. To determine the optimal temperature and pH, or the thermo- and pH-sensitivity of the mutant enzymes, 6 mg/mL lichenan (M.W.: 139,000, Sigma) was used as substrate, whereas 0.8–14 mg/mL lichenan was applied to assess the specific activity of each mutant 1,3-1,4-β-D-glucanase. Various amounts of purified enzymes (0.19–0.97 μg/mL) were used in each kinetic assay reaction, depending on the enzymatic activity of the enzyme. Enzyme activity assays were carried out in 0.3 mL reaction mixtures containing lichenan at the respective optimal pH of each enzyme, which was prepared with 50 mM sodium citrate (pH 6.0), sodium phosphate (pH 7.0) or Tris-HCl (pH 8.0) buffer. After incubation at an optimal temperature for 10 min, the enzyme reaction was terminated by the addition of 0.6 mL of a dinitrosalicylic acid reagent (1% 3,5-dinitrosalicylic acid, 0.2% phenol, 1% NaOH) [28] and incubated at 95 °C for 10 min. Finally, 0.15 mL of 40% sodium potassium tartrate solution was added to the reaction mixtures, which were then allowed to cool at an ambient temperature for 15 min, and the absorbance at 575 nm was recorded. One unit of enzyme activity was defined as the amount of enzyme required to release 1 μmol of reducing sugar (glucose equivalent). The specific activity was expressed in micromoles of glucose per minute per milligram of protein. Kinetic data were analyzed using the computer software ENZFITTER (BIOSOFT).

Table 2
Kinetic properties of wild-type and mutant forms of *F. succinogenes* 1,3-1,4-β-D-glucanase

Enzyme	Specific activity[a] unit/mg	k_{cat} s^{-1}	K_M, lichenan mg/ml	k_{cat}/K_M $s^{-1}(mg/ml)^{-1}$	$\Delta\Delta G_b$[b] kcal/mol
Wild type	2065±82	1296±51	2.50±0.09	518	–
K200F	1817±169	1141±106	2.54±0.00	449	0.153
K200M	1452±11	911±7	1.99±0.02	458	0.139
G201S	2155±53	1353±33	3.98±0.12	340	0.386
D202L	1406±91	883±57	2.02±0.02	436	0.171
D202N	4081±253	2562±159	2.71±0.08	944	−0.385
W203F[c]	8726±147	5476±92	4.37±0.14	1253	−0.425
W203R[c]	70±0	44±0	17.32±0.03	2.5	3.441
T204F	2034±115	1277±72	5.42±0.05	236	0.614
F205L	1377±54	865±34	6.29±0.36	137	0.949
D206M	3282±178	2060±112	3.68±0.10	559	−0.049
D206N	2962±136	1860±85	2.34±0.06	796	−0.275
D206R	1114±2	699±1	1.44±0.01	486	0.041
G207N	3115±104	1955±65	26.71±1.23	74	1.255
G207–	969±2	608±1	5.72±0.03	106	1.108
N208G	1501±71	942±44	6.02±0.19	157	0.868
R209M	1652±28	1037±18	1.89±0.10	549	0.025

[a] Reactions were performed with lichenan used as the substrate in 50 mM sodium citrate buffer (pH 6.0), 50 mM sodium phosphate buffer (pH 7.0) or 50 mM Tris–HCl buffer (pH 8.0), and at optimal temperatures for the individual enzymes as characterized in this study. The optimal temperature was 40 °C for G201S, T204F, F205L, G207– and N208G, 45 °C for K200F, K200M, D202L and R209M, and 50 °C for the rest mutant enzymes. The optimal pH was 6 for G201S, D202L, T204F, F205L, D206R, G207– and N208G mutant enzymes, and pH 8 for the rest mutant enzymes.

[b] $\Delta\Delta G_b$: comparative binding energy of wild-type and mutant enzymes with substrate lichenan. $\Delta\Delta G_b = -RT \ln\{(k_{cat}/K_M)_{mut}/(k_{cat}/K_M)_{wt}\}$.

[c] Data obtained from Cheng et al. [24].

2.6. Fluorescence spectrometry

The fluorescence emission spectra of native, 8 M urea-denatured, and denatured-renatured wild-type and mutant forms of Fsβ-glucanase were collected on an AMICO-Bowman Series 2 spectrofluorimeter (Spectronic Instruments, Inc., NY) with a 10×10-mm quartz cuvette at 25 °C. All the protein samples were analyzed at 20 μg/mL in 50 mM SPB (pH 7.0) in the presence or absence of 8 M urea. The urea-denatured samples were then renatured by dialysis against 50 mM SPB (pH 7.0) at 4 °C for 24 h. Emission spectra were recorded from 310 to 430 nm by excitation at 295 nm, with use of a 4-nm monochromator bandpass.

2.7. Structural modeling analysis

The crystal structures of truncated 1,3-1,4-β-D-glucanase (TFsβ-glucanase) [21] and TFsβ-glucanase in complex with its product β-1,3-1,4-cellotriose (CLTR) [25] were used for creating model structures of mutant enzymes. Manual rebuilding of the model for specific mutant enzyme was performed by use of the TURBO-FRODO program [29], and mutant enzyme model structures were further energy minimized by use of a CNS program (http://cns.csb.yale.edu/v1.1/).

3. Results

3.1. Expression and purification of mutant forms of Fsβ-glucanase

The wild-type and 14 mutant Fsβ-glucanases, namely K200F, K200M, G201S, D202L, D202N, T204F, F205L, D206M, D206N, D206R, G207N, G207−, N208G and R209M, were effectively expressed in *E. coli* BL21 (DE3) host cells upon induction with 1 mM IPTG at 33 °C. All the Fsβ-glucanases containing a *pel* leader sequence at the N terminus and a His-tag at the C terminus were expressed extracellularly into culture medium and efficiently purified with use of a Ni-NTA affinity column. As judged by SDS-PAGE and zymography analysis, the purity of each purified mutant Fsβ-glucanase was greater than 95% homogeneity with one distinct band per enzyme preparation (data not shown).

3.2. Temperature and pH effects on enzymatic activity of wild-type and mutant Fsβ-glucanases

The effects of temperature and pH on the enzymatic activity of the purified mutant enzymes were examined. The optimal temperature of mutant Fsβ-glucanases were between 40 °C and 50 °C, and an optimal pH of 6 or 8 was observed. Further, the temperature and pH sensitivity of the mutant Fsβ-glucanases were investigated to characterize the influence of introduced mutated amino-acid residues. Fig. 2A shows the effect of temperature on the enzymatic activity of wild-type and some mutant glucanases. All the mutant enzymes with below 40 °C treatment had similar relative enzymatic activities (90–110%) to enzymes not heat treated. Significant differences in heat sensitivity among wild-type and mutant Fsβ-glucanases were observed upon their treatment at 45–50 °C. After pre-treatment at 45 °C for 10 min, the wild-type and most of the mutant glucanases could maintain more than 85% of their original activity; however, K200M, T204F, D206M and D206N enzymes lost 30–43% of activity, and K200F, 72%. When incubated at 50 °C for 10 min, D202L, D206R and G207-retained 56–71% activity, whereas the wild type showed only 38% of its original activity. Less than 14% enzymatic activity was detected for K200F (14%), K200M (14%), T204F (5%), F205L (8%), D206M (13%), D206N (10%) and G207N (4%) mutant enzymes. Upon heat treatment at ≥55 °C for 10 min, less than 14% enzymatic activity was detected for all of the mutant enzymes (Fig. 2A). G201S, D202N, N208G and R209M mutant enzymes exhibited overall profiles of relative enzymatic activity similar to that of the wild-type enzyme after incubation at temperatures ranging from 30 to 70 °C for 10 min (data not shown).

The effect of pH on the enzymatic activity of the wild type and some mutant glucanases is shown in Fig. 2B. All the mutant enzymes exhibited similar pH response profiles in terms of their activities between pH 4 and pH 10 to that of the wild-type Fsβ-glucanase. Overall, the stability of wild-type and mutant enzymes decreased at pH values lower than 4. Most enzymes retained less than 20% of their activities at pH ≤3, except D202L, F205L, and N208G mutant enzymes, which retained 35–40% of their original enzymatic activities at pH 3.

3.3. Kinetic analysis of wild-type and mutant forms of Fsβ-glucanase

The catalytic properties of mutant enzymes were kinetically evaluated by determination of their enzymatic activities under optimal pH and temperature, with lichenan used as the substrate (Table 2). D202N, D206M, and D206N enzymes showed a 1.4- to 2.0-fold increase in k_{cat} in comparison to the wild-type glucanase. The catalytic efficiencies (k_{cat}/K_M) of D202N and D206N were also 1.8- and 1.5-fold, respectively, higher than that of the wild-type enzyme. In contrast, the replacement of Asp202 with Leu or replacement of Asp206 with Arg caused a slight decrease (~1.2-fold) in the catalytic efficiency of the enzyme. Deleting or mutating Gly207 caused a significant effect on catalytic efficiency of the enzyme. Although a slight increase in k_{cat} was found in G207N, the catalytic efficiency of G207N and G207− was decreased 7.0- and 4.9-fold, respectively, due to a 10.7- and 2.3-fold increase in K_M for lichenan. These results indicate that Asp202, Asp206 and Gly207 residues play a role in the catalysis of Fsβ-glucanase.

Table 3
The interactions of amino acid residues located in the C-terminal of strand β13 and in the connecting loop between strands β13 and β14 with their neighboring residues in *F. succinogenes* 1,3-1,4-β-D-glucanase

Residue	Interactions[a]	Possible effects after mutation
Hydrogen bonding		
Lys200	Nζ-O-Asp214 (3.31) –O-Ile217 (2.82) –H_2O (2.9~3.0)	H-bonds were abolished in K200F and K200M mutants
Gly201	Not observed	Trp203 in G201S may be squeezed toward the concave side, thus affecting substrate binding
Asp202	Oδ2-N-Met1 (2.68) –O-Met1 (3.44)	Asn202 in D202N may serve as a proton donor, thereby strengthening the H-bond network
Trp203	Ne1-O6 (subsite −2 of substrate) (2.92)	W203F still holds the stacking interaction with the substrate -3
Thr204	Oγ1-Nζ-Lys5 (2.81) –N-Phe205 (2.90) –O-Val210 (2.63)	Replacement of Thr with Phe led to a breakdown of the hydrogen bond network
Asp206	Oδ1-H_2O (3.1~3.6) Oδ2-H_2O (3.6)	D206N mutant retained the Type II turn geometry, while H-bonds were abolished in D206M and D206R
Gly207	N-Oε -Glu144 (3.40) O-N-Glu144 (2.82) –H_2O (3.5)	Gly207, a key residue in the type II β turn, has hydrogen bonds with Glu144. Mutation on Gly207 may affect the structure of the type II β turn and Glu144 loop, leading to a negative effect on structural packing and substrate binding.
Asn208	Nδ2-O-Val210 (3.44) Oδ1-N-Ser142 (3.89) –O-Ser142 (3.33) –N-Val210 (2.95) –O-Val210 (3.39)	Hydrogen bonds were lost in the N208G mutant, leading to decreased structural stability of enzyme-substrate
Arg209	Nε-Oγ-Ser42 (3.65) Nη1-Oε -Glu154 (3.86) –H_2O (2.9) Nη2-H_2O (2.6~4.0)	Arg209 residue located on the protein surface; any replacement may contribute only minor effects on the local structural geometry of the enzyme
van der Waals		
Phe205	Trp141(3.88) Sugar ring of substrate	The van der Waals interactions were lost in the Phe205 mutant
Asn208	Trp141(3.60)	The van der Waals interaction in the N208G mutant was lost

[a] Observed interactions in the three-dimensional structures of TFsβ-glucanase and Fsβ-glucanase–CLTR complex (distance (Å) in parentheses).

A substantial reduction in substrate binding affinity was observed in T204F, F205L and N208G mutant enzymes, with a 2.2-, 2.5- and 2.4-fold increase in K_M relative to the wild-type Fsβ-glucanase. Because of a slight decrease in k_{cat}, T204F, F205L and N208G enzymes were catalytically less efficient (2.2- to 3.8-fold lower in k_{cat}/K_M value) than the wild-type enzyme. Mutation of residues 200, 201 or 209 had a negligible effect on k_{cat} or K_M values. These results indicate that amino acid residues Thr204, Phe205 and Asn208 are important for enzyme–substrate binding.

3.4. Comparative binding energies of wild-type and mutant enzymes

The difference in enzyme–substrate binding energies between the wild-type and specific mutant Fsβ-glucanases were investigated to evaluate the possible contribution(s) of the side-chain groups of specific amino acids to enzyme-substrate binding. The apparent contributions, represented as $\Delta\Delta G_b$ values, of the side chains of different amino acids to the binding energy of the enzyme–transition state complex were calculated as reported previously [30,31]. $\Delta\Delta G_b$ is given by the equation

$$\Delta\Delta G_b = -RT \ln \{(k_{cat}/K_M)_{mut}/(k_{cat}/K_M)_{wt}\},$$

where mut and wt refer to mutant and wild-type enzymes, respectively. The binding energy can be referred to the stability and complementarity of enzyme-substrate and enzyme–transition state complexes [32]. In the present study, we found a 2.2- to 10.7-fold increase in K_M for T204F, F205L, G207N, G207− and N208G enzymes, which, accompanied by comparative binding energy values ($\Delta\Delta G_b$) from 0.614 to 1.255 kcal/mol, indicated that the interactions between the side chains of Thr204, Phe205, Gly207and Asn208 and the substrate were lost or weaker in the mutant enzyme–substrate complexes. This situation was also the case for the G201S mutant, with $\Delta\Delta G_b$=0.386 kcal/mol and a 1.6-fold increase in K_M relative to the wild-type enzyme. Marginal decrease in specific activities of K200F, K200M, D202L, D206R and R209M also coincided with slightly lower $\Delta\Delta G_b$ values (0.025 ~ 0.171 kcal/mol) relative to the wild-type enzyme. In contrast, a negative binding energy change (−0.049 ~ −0.385 kcal/mol) accompanied by an increased k_{cat} (1.4- to 2.0-fold) was found for D202N, D206M and D206N enzymes, which implied that the binding energy in the mutants was perhaps used to stabilize the enzyme–transition state complex and consequently enhanced the catalytic efficiency of the enzymes.

3.5. Fluorescence spectrometric analysis of wild-type and mutant Fsβ-glucanases

The emission fluorescence spectra of the native, urea-denatured, and denatured-renatured wild-type and mutant forms of the Fsβ-glucanases were analyzed. Fig. 3 shows the superimposed emission spectra of the native form of the wild-type and selected mutant enzymes (D202L, F205L, and N208G) with a maximum emission peak at 333 nm. The emission spectra of 8 M urea-denatured wild-type and mutant enzymes showed a bathochromic (red) shift with a maximum peak at 349 nm and a slight shoulder at 376 nm. All of the urea-denatured enzymes were dialyzed against 50 mM SPB (pH 7.0) to remove the denaturant, and then analyzed for their fluorescence emission spectra under experimental conditions identical to those employed for the native and urea-denatured protein samples. The data in Fig. 3 show that after refolding, the maximum emission spectra of the renatured wild-type and selected mutant enzymes all shifted back to 333 nm and superimposed well with each other, with only a minor difference (<±4%) on the maximal absorbance at peak 333 nm. Similar results were obtained for other mutant forms of Fsβ-glucanase in this study (data not shown) and for the W203F mutant published previously [24]. Enzymatic activities of the native and renatured wild-type and mutant Fsβ-glucanases were also determined in parallel. Approximately 91–100% activity, relative to the native enzyme, was recovered for the renatured enzymes. These results suggest that none of the amino acid mutations to the Fsβ-glucanase in this study caused global conformational change or aberrant folding of the enzyme. Therefore, the observed differences in the kinetic properties between the wild-type and mutant forms of Fsβ-glucanase apparently are not due to the disruption of the structural integrity of the enzyme.

4. Discussion

F. succinogenes 1,3-1,4-β-D-glucanase (Fsβ-glucanase) is the only natural circularly permuted enzyme in the family of 16 glycosyl hydrolases [20]. On the basis of amino acid sequence alignment, structural modeling, and X-ray structural studies (Fig. 1) [21], we observed that the structure of TFsβ-glucanase, while similar to the fold of many glycosyl hydrolases and carbohydrate-binding modules, has differences in its connecting loops and random coils as compared to its *Bacillus* counterparts [21,33]. Most interestingly, we found an overlapping region, with a very low amino acid similarity (Fig. 1B), on the surface top of the concave side, which is proposed to be the substrate binding cleft in the glucanases from *F. succinogenes* and *B. licheniformis*. We investigated here whether the specific amino acid residues (residues 200–209) in the corresponding region (*i.e.*, β-strand 13-loop-β-strand 14 of *F. succinogenes*), can contribute to the catalytic function of the enzyme. Fourteen mutant enzymes were successfully created and transformed into *E. coli* host cells and had a protein expression level similar to that of the recombinant wild-type enzyme. No discernible differences were observed between the secondary structures of the homogeneous prepared wild-type and mutant forms of Fsβ-glucanase (Fig. 3). The specific bonding or interactions between residues 200–209 and their neighboring molecules in the wild-type and mutant Fsβ-glucanases were summarized (Table 3) on the basis of the three-dimensional structures [21,25] and structural modeling analysis of TFsβ-glucanase and TFsβ-glucanase–CLTR complex in this study. In combination with the results obtained from kinetic studies, we demonstrate that specific amino acids on the surface top of the concave side indeed play a role in the enzyme's catalytic function.

In the present study, we observed opposite effects on the catalytic activity of Fsβ-glucanase when residue Asp202 was substituted with Asn and Leu. A 1.5-fold decrease and a 2.0-fold increase in specific activity were found for D202L and D202N, respectively, as compared

Fig. 4. Stereo views of the superimposition of TFsβ-glucanase (PDB entry: 1mve) and TFsβ-glucanase–CLTR (subsite −3 to −1) complex (PDB entry: 1zm1). (A) Stereo view of the superimposition of residues 202 to 209 of TFsβ-glucanase (blue) and TFsβ-glucanase–CLTR (subsite −3 to −1 from left to right, green and red) complex (pink). Hydrogen bonds are shown in dotted lines. Two residues (*i.e.*, Trp203 and Thr204), in the targeted studied region were found to directly interact with the sugar. The Nε of Trp203 interacts with the O6 of subsite −2, and the carbonyl O of Thr204 interacts with the O6 of subsite −1. Phe205 also showed stacking interaction with the subsite −2 of CLTR. (B) Superimposition of the structural region around Phe205 in the TFsβ-glucanase–CLTR (pink) and mutant F205L (yellow, structural model). The subsite −2 of CLTR is sandwiched in between aromatic residues Phe205 and Tyr42 via π–π stacking interactions in the complex structure. Replacement of Phe205 with leucine may break down the interactions with CLTR. (C) Superimposition of the structural region around Gly207 in TFsβ-glucanase–CLTR (pink), mutant G207N (orange) and G207− (blue). In the complex structure, the main chain atoms O and N of G207 have hydrogen bonds with the main chain N and the side-chain Oε2 of E144, respectively. In the mutant modeling structure G207N, the hydrogen bond between the main chain atom N of G207 and the side-chain Oε2 of E144 is not present, whereas the hydrogen bond is broken down in the G207-deletion mutant. (D) Superimposition of the structural region around Asn208 in the TFsβ-glucanase–CLTR (pink) and mutant N208G (green). In the TFsβ-glucanase–CLTR enzyme complex, the residue Asn208 is located at the β-turn and its side-chain atoms of Oδ1 and Nδ2 have hydrogen bonds with the main chain of Ser142 and Val210. This side-chain is absent in the mutant Gly208, and no hydrogen bond appeared.

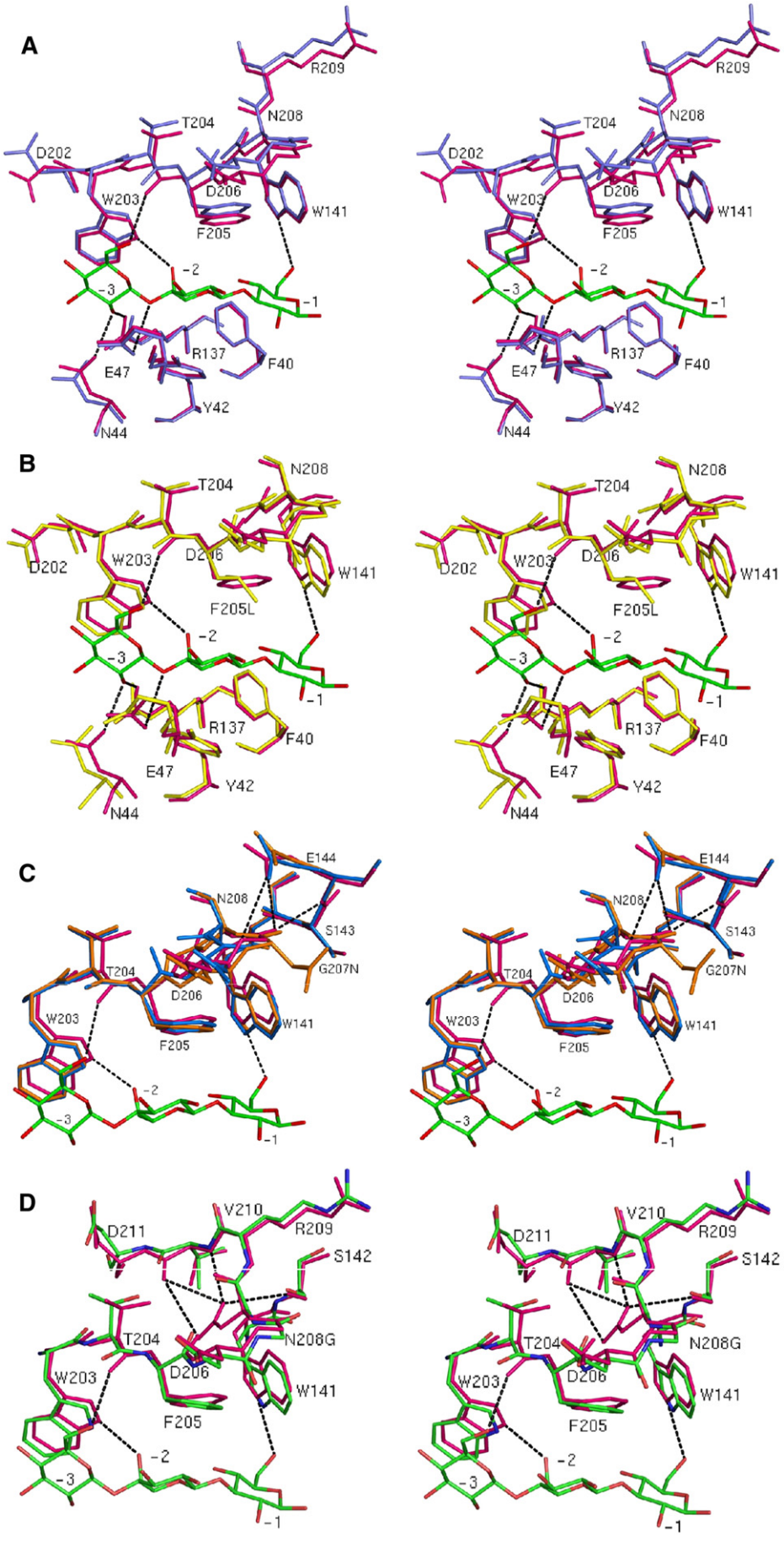
A
R209
N208
T204
D202
W203
D206
W141
F205
-2
-3
-1
R137
E47
F40
Y42
N44
B
N208
T204
D202
W203
D206
W141
F205L
-2
-3
-1
R137
F40
E47
Y42
N44
C
E144
N208
S143
T204
G207N
D206
W203
W141
F205
-2
-3
-1
D
V210
D211
R209
S142
T204
N208G
W203
D206
W141
F205
-2
-3
-1

with the wild-type enzyme (Table 2). A negative (−0.385 kcal/mol) and a positive (0.171 kcal/mol) binding energy were also observed for D202N and D202L, respectively. These results suggest a stronger enzyme–substrate interaction in D202N mutant than in the wild-type enzyme that can be correlated to the superior catalytic efficiency observed in the mutant enzyme (Table 2). Similar phenomena were observed in W203F and W203R mutant enzymes. Our previous study demonstrated that Trp203 residue located at the C-terminal end of strand β13 of Fsβ-glucanase is crucial for enzymatic activity and for binding with the substrate [24]. A negative (−0.425 kcal/mol) and a positive (3.441 kcal/mol) binding energy were observed in the W203F and W203R, respectively, which correlated well with the observed increase (2.4-fold) and decrease (207-fold) in the catalytic efficiency of the W203F and W203R enzymes, respectively (Table 2) [24]. Our structural model shows that, in the G201S mutant, the bigger side chain of serine compared to that of glycine could squeeze Trp203 slightly toward the concave side, thus narrowing the substrate binding cleft on the concave side of the β-jellyroll structure and leading to a slightly unfavorable environment for substrate binding. This finding may be why a 1.6-fold increase in K_M and 0.386 kcal/mol of binding energy lost was observed for the G201S mutant enzyme relative to the wild-type glucanase.

Aspartic acid 206 cooperates with Phe205, Gly207, and Asn208 to form a Type II turn located at the top of the concave region in Fsβ-glucanase (Fig. 1A). Both the Oδ1 and Oδ2 atoms of Asp206 was observed to make hydrogen bonds with two water molecules in which the Oδ1 atom is indirectly connected to the Nζ atom of Lys5 via a water molecule. The Type II turn configuration may be stabilized by these hydrogen bonds. In comparison with the free-form TFsβ-glucanase structure (PDB entry: 1 mve) [21], the protein folding of TFsβ-glucanase–CLTR complex showed a significant conformational change in loop residues 203–209 [25] (Fig. 4A). Therefore, the loop region was suggested to possibly play a role as a gate of the active site in the enzyme that provides a good fit and tight binding for the substrate. When the Asp206 residue was mutated into asparagine, the hydrogen bonding with water molecules in the D206N mutant enzyme was retained and a better molecular interaction observed ($\Delta\Delta G_b$= −0.275 kcal/mol), with a 1.54-fold increase in catalytic efficiency in D206N than in the wild-type enzyme (Table 2). In contrast, when Asp206 was replaced with methionine or arginine, the hydrogen bonds found in wild-type glucanase were not present in the structural model of the mutants (data not shown). The abolishment of hydrogen bonding might result in the conformation of the Type II turn and/or the connecting loop between strands β13 and β14 becoming more flexible and less stable. Therefore interesting kinetic results were obtained for D206M and D206R mutants; opposite effects on the k_{cat} of the enzyme were found (Table 2).

Our previous studies showed that the enzyme–substrate/product (CLTR) complex structure of Fsβ-glucanase was stabilized by numerous hydrogen bonds between CLTR and residues, including Trp141, Trp203 and Thr204, and van der Waals stacking interactions between CLTR and residues such as Trp203 and Phe205 [25]. We also observed that mutation on residues Trp141 and Trp203, which bind directly with the subsites −1 and −2, respectively, of the sugar product CLTR (Fig. 4A), resulted in a 1.7- to 6.9-fold increase in K_M of Fsβ-glucanase (Table 2) [24]. Here, replacement of Thr204 with Phe, or Phe205 with Leu was also found to cause a 2.2- to 2.5-fold increase in K_M. Thr204 is the last residue on strand β13 of Fsβ-glucanase, and the Oγ1 of Thr204 forms three hydrogen bonds with the Nζ atom of Lys5, the main chain NH of Phe205, and the main chain of Val210 (O atom) [25]. The structure of TFsβ-glucanase–CLTR also reveals that the main chain of Thr204 (O atom) directly interacts with subsite −3 of the oligosaccharide (Fig. 4A). In this study, when Thr204 residue was mutated to phenylalanine, the larger side chain of Phe might be too big to fit into the space originally occupied by the Thr residue and led to a breakdown of the hydrogen bond network between Thr204 and its contiguous residues Lys5, Phe205 and Val210. In addition, the loop-region connecting strands β13 and β14 may therefore have a subtle change in T204F, leading to the 0.614 kcal/mol loss in binding energy in the T204F mutant relative to the wild-type Fsβ-glucanase. Consequently, the enzyme–substrate binding was less effective (2.2-fold increase in K_M value) in T204F. In the crystal structure of TFsβ-glucanase–CLTR, the aromatic ring of Phe205 clamped the subsite −2 of the β-1,3-1,4-cellotriose (CLTR) with Tyr42 via a van der Waals interaction [25]. In addition, the aromatic ring of Phe205 was perpendicular to Trp141 at a distance of about 3.88 Å (Fig. 4B), which may also help Trp141 maintain an optimal local configuration through van der Waals interactions. When Phe205 was replaced by leucine, the interaction of the phenylalanine aromatic ring with the sugar ring of CLTR or with Trp141 was abolished (Fig. 4B). The binding energy ($\Delta\Delta G_b$) in the F205L mutant enzyme was also reduced by 0.949 kcal/mol, which may have contributed to attenuating the structural stability of the enzyme–substrate complex. As a result, a significant decrease in catalytic efficiency (3.8-fold) was observed in the F205L mutant relative to that of the wild-type enzyme (Table 2).

Mutation on Gly207 caused a significant negative effect on substrate binding affinity. The main chain atoms O and N of Gly207 have hydrogen bonds with the main chain atom N and the side-chain atom Oε2 of Glu144, respectively (Fig. 4C). The left Gly207 loop between strands β13 and β14 and the right Glu144 loop between strand β10 and α2 are located together at the top of the concave region of Fsβ-glucanase (Fig. 1A). Our structural model suggests that in the G207N mutant, the polar side chain of Gln207 might protrude into the concave site, resulting in disturbing the substrate binding to the active site cavity (Fig. 4C). Or, the Oδ1 and Nδ2 atoms of Gln207 located on the loop surface might have more freedom to move around and interact with the residues Ser143, Glu144 and Ser145 and subsequently caused the Glu144 loop to be unstable or have a subtle conformational change. Therefore, the G207N mutant enzyme has a much higher K_M value (10.7-fold increase) than the wild-type enzyme. In the structure model of the Gly207 deletion mutant (G207−), the hydrogen bonds of the key Type II turn residue 207 with the neighboring amino acid residues all disappeared (Fig. 4C). This situation might cause the left Gly207 loop to recoil and the right Glu144 loop to shift away, and thus the catalytic efficiency of the enzyme was significantly affected. The Nδ2 and Oδ1 atoms of Asn208, another residue located at the β-turn loop connecting strands β13 and β14, have hydrogen bonds interacting with the main chain of residues Val210 and Ser142 (Fig. 4D, Table 3). The side chain of Asn208 also interacts with Trp141 via a van der Waals interaction. When Asn208 was mutated to glycine, all the hydrogen bonds were abolished and the smaller size of glycine may have led to an increase in the structural flexibility of Trp141. The structural geometry at Ser142, Trp141, and the β-turn loop in the N208G mutant enzyme could have thus been affected, leading to a decrease in structural stability of the enzyme–substrate or enzyme–transition state complex. This situation could explain the loss of 0.868 kcal/mol in the binding energy of N208G relative to the wild-type enzyme, in turn, accompanied by a 2.4-fold increase in K_M and a slight decrease (1.4-fold) in k_{cat} of the enzyme (Table 2).

In summary, the present study demonstrates the structural and functional relations of the amino acid residues Lys200–Arg209 in *F. succinogenes* 1,3-1,4-β-D-glucanase. By using site-directed mutagenesis, initial rate kinetics, enzyme-transition state theory, and structural modeling analysis, we showed the residues Phe205, Gly207, and Asn208 located at the β-turn loop connecting strands β13 and β14 to play some role in the catalysis of Fsβ-glucanase. Replacement of Asp by Asn at residue 202 can result into a 1.98-fold increase in specific activity of the enzyme.

Acknowledgments

This study was supported in part by Grant NSC 93-2313-B-001-101 from the National Science Council and by Academia Sinica, Taipei, Taiwan, R.O.C.

References

[1] G. Davies, B. Henrissat, Structures and mechanisms of glycosyl hydrolases, Structure 3 (1995) 853–859.
[2] M.A. Anderson, B.A. Stone, A new substrate for investigating the specificity of β-glucan hydrolases, FEBS Lett. 51 (1975) 202–207.
[3] J.R. Woodward, G.B. Fincher, B.A. Stone, Water-soluble (1→3),(1→4)-β-D-glucans from barley (*Hordeum vulgare*) endosperm. II. Fine structure, Carbohydr. Polym. 3 (1983) 207–225.
[4] A. Planas, Bacterial 1,3-1,4-β-glucanases: structure, function and protein engineering, Biochim. Biophys. Acta 1543 (2000) 361–382.
[5] N. Murphy, D.J. McConnell, B.A. Cantwell, The DNA sequence of the gene and genetic control sites for the excreted *B. subtilis* enzyme β-glucanase, Nucleic Acids Res. 12 (1984) 5355–5367.
[6] E. Hinchliffe, Cloning and expression of a *Bacillus subtilis* endo-1,3-1,4-β-D-glucanase gene in *Escherichia coli* K12, J. Gen. Microbiol. 130 (1984) 1285–1291.
[7] M.E. Louw, S.J. Reid, T.G. Watson, Characterization, cloning and sequencing of a thermostable endo-(1,3-1,4) β-glucanase-encoding gene from an alkalophilic *Bacillus brevis*, Appl. Microbiol. Biotechnol. 38 (1993) 507–513.
[8] R. Borriss, K. Buettner, P. Maentsaelae, Structure of the beta-1,3-1,4-glucanase gene of *Bacillus macerans*: homologies to other beta-glucanases, Mol. Gen. Genet. 222 (1990) 278–283.
[9] J. Hofemeister, A. Kurtz, R. Borriss, J. Knowles, The β-glucanase gene from *Bacillus amyloliquefaciens* shows extensive homology with that of *Bacillus subtilis*, Gene 49 (1986) 177–187.
[10] J. Lloberas, J.A. Perez-Pons, E. Querol, Molecular cloning, expression and nucleotide sequence of the endo-β-1,3-1,4-D-glucanase gene from *Bacillus licheniformis*. Predictive structural analyses of the encoded polypeptide, Eur. J. Biochem. 197 (1991) 337–343.
[11] R.M. Teather, J.D. Erfle, DNA sequence of a *Fibrobacter succinogenes* mixed-linkage β-glucanase (1,3-1,4-β-D-glucan 4-glucanohydrolase) gene, J. Bacteriol. 172 (1990) 3837–3841.
[12] H.J. Flint, J. Martin, C.A. McPherson, A.S. Daniel, J.X. Zhang, A bifunctional enzyme, with separate xylanase and β(1,3-1,4)-glucanase domains, encoded by the *xynD* gene of *Ruminococcus flavefaciens*, J. Bacteriol. 175 (1993) 2943–2951.
[13] S. Schimming, W.H. Schwarz, W.L. Staudenbauer, Properties of a thermoactive β-1,3-1,4-glucanase (lichenase) from *Clostridium thermocellum* expressed in *Escherichia coli*, Biochem. Biophys. Res. Commun. 177 (1991) 447–452.
[14] G.B. Fincher, P.A. Lock, M.M. Morgan, L. Lingelbach, R.E.H. Wettenhall, J.F.B. Mercer, A. Brandt, K.K. Thomsen, Primary structure of the (1→3,1→4)-β-D-glucan 4-glucohydrolase from barley aleurone, Proc. Natl. Acad. Sci. U. S. A. 83 (1986) 2081–2085.
[15] J.C. Litts, C.R. Simmons, E.E. Karrer, N. Huang, R.L. Rodriguez, The isolation and characterization of a barley 1,3-1,4-β-glucanase gene, Eur. J. Biochem. 194 (1990) 831–838.
[16] U. Helmut, Industrial Enzymes and their Applications, John Wiley & Sons, New York, 1998.
[17] B.A. Stone, A.E. Clarke, Chemistry and Biology of 1,3-β-Glucans, La Trobe Univ. Press, Bundoora, 1992.
[18] W.B. White, H.R. Bird, M.L. Sunde, J.A. Marlett, Viscosity of beta-D-glucan as a factor in the enzymatic improvement of barley for chicks, Poult. Sci. 62 (1983) 853–862.
[19] S. Schimming, W.H. Schwarz, W.L. Staudenbauer, Structure of the *Clostridium thermocellum* gene-*licB* and the encoded β-l,3-1,4-glucanase — a catalytic region homologous to *Bacillus lichenases* joined to the reiterated domain of clostridial cellulases, Eur. J. Biochem. 204 (1992) 13–19.
[20] U. Heinemann, M. Hahn, Circular permutations of protein sequence: not so rare? Trends Biochem. Sci. 20 (1995) 349–350.
[21] L.-C. Tsai, L.-F. Shyur, S.-H. Lee, S.-S. Lin, H.-S. Yuan, Crystal structure of a natural circularly permuted jellyroll protein: 1,3-1,4-β-D-glucanase from *Fibrobacter succinogenes*, J. Mol. Biol. 330 (2003) 607–620.
[22] T.-N. Wen, J.-L. Chen, S.-H. Lee, N.-S. Yang, L.-F. Shyur, A truncated *Fibrobacter succinogenes* 1,3-1,4-β-D-glucanase with improved enzymatic activity and thermotolerance, Biochemistry 44 (2005) 9197–9205.
[23] J.-L. Chen, L.-J. Tsai, T.-N. Wen, J.-B. Tang, H.-S. Yuan, L.-F. Shyur, Directed mutagenesis of specific active site residues on *Fibrobacter succinogenes* 1,3-1,4-β-D-glucanase significantly affects catalysis and enzyme structural stability, J. Biol. Chem. 276 (2001) 17895–17901.
[24] H.-L. Cheng, L.-C. Tsai, S.-S. Lin, H.-S. Yuan, N.-S. Yang, S.-H. Lee, L.-F. Shyur, Mutagenesis of Trp^{54} and Trp^{203} residues on *Fibrobacter Succinogenes* 1,3-1,4-β-D-glucanase significantly affects catalytic activities of the enzyme, Biochemistry 41 (2002) 8759–8766.
[25] L.-C. Tsai, L.-F. Shyur, Y.-S. Cheng, S.-H. Lee, Crystal structure of truncated *Fibrobacter succinogenes* 1,3-1,4-β-D-glucanase in complex with β-1,3-1,4-cellotriose, J. Mol. Biol. 354 (2005) 642–651.
[26] M. Hahn, J. Pons, A. Planas, E. Querol, U. Heinemann, Crystal structure of *Bacillus licheniformis* 1,3-1,4-β-D-glucan 4-glucanohydrolase at 1.8 Å resolution, FEBS Lett. 374 (1995) 221–224.
[27] J. Pons, E. Querol, A. Planas, Mutational analysis of the major loop of *Bacillus* 1,3-1,4-β-D-glucan 4-glucanohydrolases, J. Biol. Chem. 272 (1997) 13006–13012.
[28] G.L. Miller, Use of dinitrosalicylic acid reagent for determination of reducing sugar, Anal. Chem. 31 (1959) 426–428.
[29] A. Roussel, C. Cambillau, The TURBO-FRODO graphics package, Graphics Geometry Partners Directory, Vol. 81, Silicon Graphics, Mountain View, CA, 1992.
[30] A.J. Wilkinson, A.R. Fersht, D.M. Blow, G. Winter, Site-directed mutagenesis as a probe of enzyme structure and catalysis: tyrosyl-tRNA synthetase cysteine-35 to glycine-35 mutation, Biochemistry 22 (1983) 3581–3586.
[31] A.R. Fersht, J.P. Shi, J. Knill-Jones, D.M. Lowe, A.J. Wilkinson, D.M. Blow, P. Brick, P. Carter, M.M. Waye, G. Winter, Hydrogen bonding and biological specificity analyzed by protein engineering, Nature 314 (1985) 235–238.
[32] A. Fersht, Structure and Mechanism in Protein Science: A Guide to Enzyme Catalysis and Protein Folding, W.H. Freeman and Company, New York, 1999.
[33] T. Keitel, O. Simon, R. Borriss, U. Heinemann, Molecular and active-site structure of a *Bacillus* 1,3-1,4-β-glucanase, Proc. Natl. Acad. Sci. U. S. A. 90 (1993) 5287–5291.
[34] G.J. Barton, ALSCRIPT-A tool to format multiple sequence alignments, Protein Eng. 6 (1993) 37–40.